engineering proceedings

Proceeding Paper

Price Dynamics and Measuring the Contagion between Brent Crude and Heating Oil (US-Diesel) Pre and Post COVID-19 Outbreak †

Claudio Marcio Cassela Inacio, Jr. *,‡ and Sergio Adriani David *,‡

Institute of Mathematics and Computer Science, University of São Paulo, Av. Trabalhador São-Carlense 400, São Carlos 13566-590, Brazil
* Correspondence: claudio.inacio@usp.br (C.M.C.I.J.); sergiodavid@usp.br (S.A.D.)
† Presented at the 8th International Conference on Time Series and Forecasting, Gran Canaria, Spain, 27–30 June 2022.
‡ These authors contributed equally to this work.

Abstract: The objective of this work is to analyze the price dynamics and the level of association between the Brent crude oil prices and heating oil (HO), i.e., US diesel. The data series are obtained from daily future contract prices of Chicago Mercantile Exchange (CME) group exchanges and the Intercontinental Exchange (ICE). A continuous evaluation of the Detrended Cross-Correlation Analysis (DCCA) between Brent crude oil prices vis-a-vis HO is proposed by means of the rolling window approach, allowing a dynamic analysis of their cross-correlations covering two periods, namely from January 2018 to December 2019 (before the COVID-19 pandemic) and from January 2020 to December 2021 (during the COVID-19 pandemic). The results indicate that there is a strong evidence of contagion in cross-correlation due to the initial impact of the pandemic, but the HO–Brent correlation fully recovered after approximately 200 days. However, lower time scales (n) are also sensitive to supply shortages in the short term and can be most reliable for agents that might not take long positions. Measuring this dynamic cross-correlation can provide useful information for investors and agents in the oil and energy markets.

Keywords: cross-correlation; DCCA method; oil derivatives; energy

Citation: Inacio, C.M.C., Jr.; David, S.A. Price Dynamics and Measuring the Contagion between Brent Crude and Heating Oil (US-Diesel) Pre and Post COVID-19 Outbreak. *Eng. Proc.* **2022**, *18*, 8. https://doi.org/10.3390/engproc2022018008

Academic Editors: Ignacio Rojas, Hector Pomares, Olga Valenzuela, Fernando Rojas and Luis Javier Herrera

Published: 21 June 2022

1. Introduction

Since the first propositions about the relationship between oil prices and economic activity proposed by Hamilton [1], a significant number of researchers have dedicated themselves to exploring the connection between variations in its price and its effects on global economic activities. According to Zhang, Lai and Wang [2], oil is a resource known for large price fluctuations, where prices increases usually cause an increase in inflation and harm the economies of importing countries. On the other hand, price drops usually cause economic recessions and political instability in exporting countries, as their economic development can be jeopardized or delayed. In addition to price levels, another relevant factor is their volatility, since a relatively small increase can cause considerable economic losses [3]. Oil price variations are influenced by several factors. The dynamics between supply and demand is one of the main factors that affect price movement, which is also sensitive to exogenous factors such as the weather and irregular events [4,5] and also to political aspects and the expectations of market agents [6,7]. Such factors make the price movement non-linear and non-stationary, which makes its analysis more challenging and an important strategy for importers, exporters, investors and governments. While crude oil prices have historically been a fundamental component of economic analysis, the variation in crude oil prices also affects a country's economy and politics [8]. For this reason, it is pertinent to understand how crude oil prices relate to its derivatives. In this context, the objective of this work is to analyze the relationship between Brent crude and heating oil (US diesel) prices, covering two periods. The first period (P1) precedes the COVID-19 crisis and includes data from January 2018 to December 2019. The second (P2) addresses the period from January 2020 to December 2021, covering the COVID-19 crisis period. The present study expands the existing literature, empirically examining the relationship between the price of oil and its derivatives in light of a continuous evaluation by means of adoption of the rolling window approach [9–11] applied to the DCCA (Detrended Cross-Correlation Analysis) method [11–20]. Such a perspective becomes relevant as the price of oil and its derivatives is the basis for decision-making in many countries. Indeed, in practical terms, the knowledge of the level of association between the prices of these products can help in the anticipation and formulation of strategies for companies and consumers. This paper is organized as follows: in Section 2, the data are introduced and the DCCA method and statistical test are presented. In Section 3, the results of the DCCA analysis are discussed. Finally, in Section 4, the main conclusions are outlined.

2. Methods

2.1. Data Characteristics

In this study, we use time series (TS) to represent daily prices of future market settlements related to the first available contract (C1) from CME group exchanges (NYMEX) and the ICE exchange for the HO and Brent, respectively. Each contract of the selected pair represents the most negotiated future contracts for diesel and crude oil worldwide. In general, price imbalances in the crude oil market tend to rapidly transfer to its derivatives. The reason is that the HO–Brent differential, also known as 'crack-spread', can be applied as a representation of the refinery margin to buy crude oil and produce diesel/heating oil.

In order to analyze the price dynamics of such pairs, we considered two distinguished periods, P_1 and P_2, where the first denotes the two-year period prior to the COVID-19 outbreak (January 18 to December 2019) and the second denotes the two-year period after the COVID-19 outbreak (January 20 to December 2021).

2.2. Detrended Cross-Correlation Analysis

In recent years, the concept of fractals in TS has been investigated by means of the Hurst exponent (H) and Auto-Regressive Fractional Integrated Moving Average (ARFIMA) processes [7,21–30]. Several computational algorithms have been proposed to explore this field [31–36]. For example, when it comes to non-stationary TS, the Detrended Fluctuation Analysis (DFA) and its respective scaling coefficients yield satisfactory results to avoid the spurious detection of correlations or self-similarity [31,32]. This process is related to the Brownian and fractional Brownian motions, which allow us to quantify the long-range dependence in the analyzed TS.

A generalization of the DFA method was proposed by Podobnik and Stanley in 2008 [37], the so-called Detrended Cross-Correlation Analysis (DCCA), which is based on the detrended covariance between two TS. This method provides the quantification of long-range cross-correlations in the presence of non-stationarity. Considering two long-range cross-correlated TS y_i and y'_i of equal length N, the values can be approached in the integrated form:

$$Y_k = \sum_{i=1}^{k} y_i \tag{1}$$

$$Y'_k = \sum_{i=1}^{k} y'_i \tag{2}$$

where $k = 1, \ldots, N$. The entire TS are fractioned into $N - n$ overlapping boxes with $n + 1$ values. The box starting at the position i and landing at the position $i + n$ is defined as the "local trend". Moreover, we can define the $\hat{Y_{k,i}}$ and $Y\hat{'}_{k,i} (i \leq k \leq i + n)$ as the ordinate points of the linear least-squares fit. For each box, it is possible to calculate the covariance of the residual as follows:

$$f^2_{DCCA}(n,i) = \frac{1}{(n-1)} \sum_{k=i}^{i+n} (Y_k - \hat{Y_{k,i}})(Y'_k - \hat{Y'}_{k,i}) \tag{3}$$

Hence, the detrended covariance is calculated by summing over all overlapping $N - n$ boxes of size n as:

$$F^2_{DCCA}(n) = \frac{1}{(N-n)} \sum_{N-n}^{i=1} f^2_{DCCA}(n,i) \tag{4}$$

When a long-range cross-correlation appears between the two TS, then $F_{DCCA} \sim n^{\lambda}$, where $\lambda \approx (H_{DFA} + H'_{DFA})/2$. The λ exponent quantifies the long-range power-law correlations, but does not quantify the level of cross-correlation [37–39]. For this matter, Zebende [39] proposed the DCCA cross-correlation coefficient, defined by:

$$\rho_{DCCA} \equiv \frac{F^2_{DCCA}}{F_{DFA}\{y_i\}} F_{DFA}\{y'_i\} \tag{5}$$

These coefficient values are interpreted similarly to Pearson's correlation and can be summarized as follows: (a) $-1 \leq \rho_{DCCA} \leq 1$, (b) $\rho_{DCCA} = 1$ for a perfect cross-correlation, (c) $\rho_{DCCA} = 0$ for no cross-correlation presented between the TS, and (d) $\rho_{DCCA} = -1$ for a perfect anti-cross-correlation.

2.3. Rolling Window Approach and the Statistical Test for $\Delta\rho_{DCCA}$

Different statistical tests have been adopted to evaluate the detrended cross-correlation coefficients [30,38,40,41]. In this work, we applied the statistical test proposed by Guedes et al. [9] to evaluate $\Delta\rho_{DCCA}$. This test allows us to analyze two distinct moments separated by a phenomenon, such as the economic crisis caused by the COVID-19 pandemic. The coefficient is represented by:

$$\Delta\rho_{DCCA}(n) = \rho^{P_2}_{DCCA}(n) - \rho^{P_1}_{DCCA}(n) \tag{6}$$

where $\rho^{P_2}_{DCCA}(n)$ and $\rho^{P_1}_{DCCA}(n)$ are the DCCA coefficients for the periods P_1 and P_2, respectively. The subsequent test consists in calculating the probability distribution function (PDF) of the $\Delta\rho_{DCCA}(n)$, supposing that they obey a normal distribution and follow the below steps [9]:

- Generate two TS with long-range cross-correlation by ARFIMA process [37];
- Divide the TS for periods P_1 and P_2 and shuffle these pairs;
- Estimate $\rho_{DCCA}(n)$ and the periods' difference $\Delta\rho_{DCCA}(n)$;
- Repeat step 2 several times;
- Obtain the distribution of $\Delta\rho_{DCCA}(n)$, and
- (Additional step) Evaluate the normality of the distribution.

In general, the PDF of $\Delta\rho_{DCCA}(n)$ converges to a normal distribution, as shown by [9]. However, we decided to conduct D'Agostino and Pearson's normality test [42,43] to verify the normality of the distribution. Hereafter, the following contagion hypothesis is tested with a T-test for the mean of the $\Delta\rho_{DCCA}(n)$ parametric group and the Wilcoxon signed-rank test for the non-parametric group:

H_0: $\Delta\rho_{DCCA}(n) = \langle\Delta\rho_{DCCA}\rangle$ (contagion does not exist);

H_1: $\Delta\rho_{DCCA}(n) \neq \langle\Delta\rho_{DCCA}\rangle$ (contagion exists);

where $\langle\Delta\rho_{DCCA}\rangle$ is the sample mean, which is approximately equal to zero. Thus, for each PDF defined by window size N (in this study, W1 = 50 days, W2 = 100 days, W3 = 150 days, W4 = 200 days, W5 = 250 days) and n time scales, we can obtain the positive critical point defined as $\Delta\rho_c(n)$ for 90%, 95%, and 99% confidence levels as follows:

$$\langle \Delta\rho_{DCCA} \rangle \pm Z_{\alpha 1/2} \frac{SD}{\sqrt{N}} \quad (7)$$

where $Z_{\alpha 1/2}$ is the value for the chosen confidence level α, SD is the standard deviation, and N is the sample size.

3. Results and Discussion

Figure 1 shows the $\rho_{DCCA}(n)$ behavior for HO–Brent during periods P_1 and P_2 for every presented time scale (n) and different sliding window sizes (W1–W5). From Figure 1a,c, one can note that considering a window size of 50 and 100 days, the prices showed a weaker relation during the beginning of 2019, which is not applied to larger sizes of W, and it is an indication of short-term effects. Moreover, we can notice that all the window sizes (W1–W5) exhibited a fall in cross-correlation in the period that preceded the COVID-19 outbreak.

Regarding the COVID-19 period (P_2), Figure 1b,d,f,h,j allow us to observe a loss of cross-correlation from March to April of 2020, when both markets presented an intense fall in prices due to lockdowns worldwide, especially the US market. Moreover, a considerable amount of market agents took a bearish (selling) position in these contracts due to the lack of global demand predictability during this period. However, one of the reasons for the price dissolution likely may have come from the specific characteristics of the diesel market. For example, heating oil—as the name suggests—can be used for heating purposes during severe US cold winters. Differently, the same product in Europe—namely gasoil—is applied for driving, such as gasoline for the US market. Therefore, during the lockdowns and with a lack of driving demand for fuel, the HO's price movement may have diverged from that of crude oil, gasoline, and gasoil.

Moreover, the 50-day and 100-day rolling windows are shown in Figure 1b,d, which showed another strong price dissolution between May and June of 2020. In addition, one can also observe that shorter window sizes are sensitive to short-term effects, which one can note during the year 2021. These effects are related to the US Gulf diesel supply shortage presented during the cold weather at the beginning of 2021 and also during the Ida hurricane effects in the second half of 2021 [44]. This might suggest that short-term supply shortages of diesel in the US Gulf can affect the HO–Brent cross-correlation, similarly to the restricted demand period caused by COVID-19. However, the supply short-term effects are not observed when using larger rolling window sizes, which is not the case for the initial pandemic effects that are displayed for every tested window. In general, the larger windows presented a cross-correlation recovery for the pair after the first half of 2020 until the end of 2021. One can also note that the greater time scales (n) diverge from the lower time scales and cannot encapsulate the complete price dynamics of both periods, since both markets are mostly interdependent in the long term compared to the short term [10].

Table 1 summarizes the descriptive statistics for the $\Delta\rho_{DCCA}$ distributions as a function of n with different sizes of W. As suggested by Guedes et al. [9], the observed mean values are approximately close to zero and the standard deviation (SD) decreases for greater W sizes. However, mostly skewness and kurtosis diverged from values observed from normal distributions, i.e., $Kurtosis \approx 3$ and $Skewness \approx 0$ for different combinations of n and W, which tends to affect the normality of the distributions. For this reason, we conducted D'Agostino and Pearson's normality test and the results are shown in Table 2. It can be seen that all the applied window sizes (W) presented non-normality for most tested time scales (n).

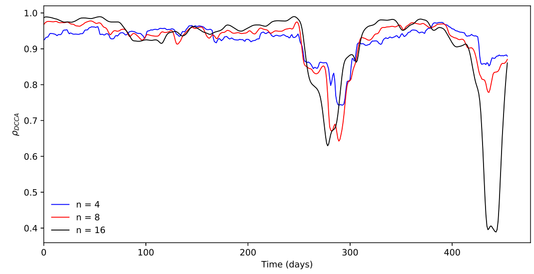

(**a**) P_1-W1

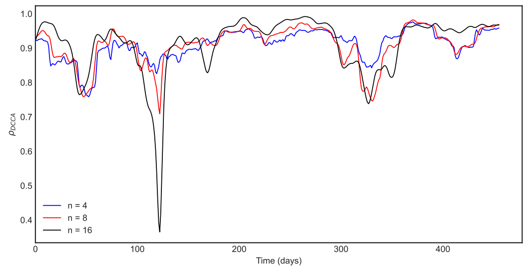

(**b**) P_2-W1

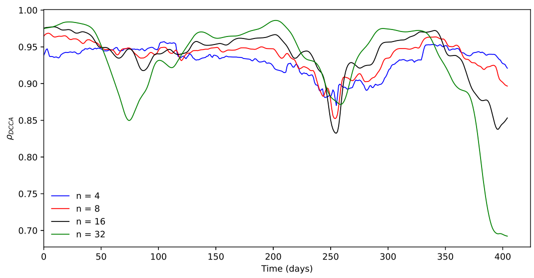

(**c**) P_1-W2

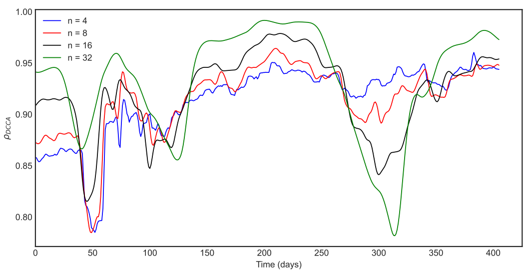

(**d**) P_2-W2

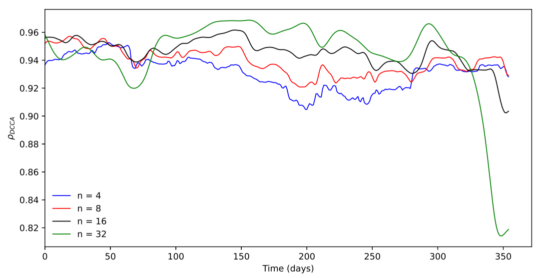

(**e**) P_1-W3

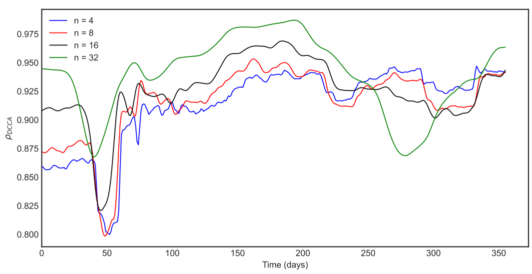

(**f**) P_2-W3

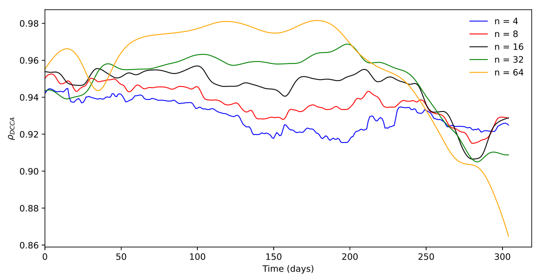

(**g**) P_1-W4

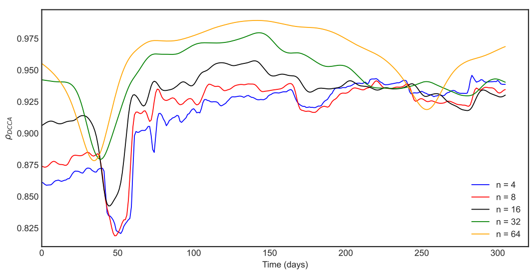

(**h**) P_2-W4

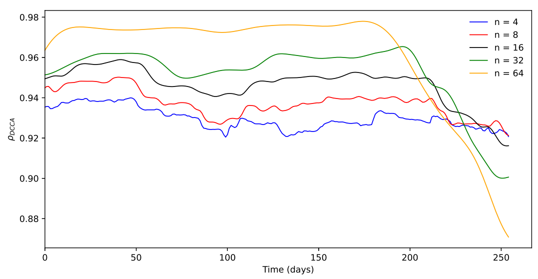

(**i**) P_1-W5

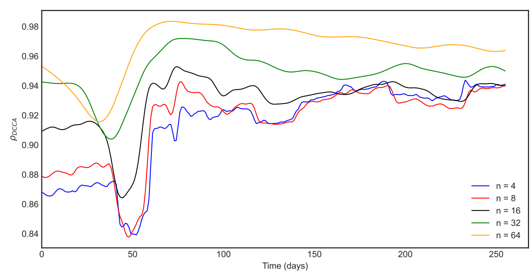

(**j**) P_2-W5

Figure 1. The Brent–HO ρ_{DCCA} TS comparison of P_1 vs. P_2 for W1 to W5.

Table 1. The *Brent-HO* descriptive summary of $\Delta\rho_{DCCA}$ for W1 to W5.

Descriptive Statistics					
Statistics	***n* = 4**	***n* = 8**	***n* = 16**	***n* = 32**	***n* = 64**
W1 = 50					
Mean	0.0469	0.0478	0.0606	-	-
SD	0.0519	0.0585	0.0949	-	-
Skewness	0.7747	1.3477	2.7715	-	-
Kurtosis	0.4957	1.3932	9.5141	-	-
W2 = 100					
Mean	0.0336	0.0314	0.0233	0.0012	-
SD	0.0513	0.0519	0.0492	0.0546	-
Skewness	0.3688	0.4340	−0.6524	−0.0903	-
Kurtosis	−0.3147	0.0274	0.0166	−0.3943	-
W3 = 150					
Mean	0.0276	0.0289	0.0216	0.0033	-
SD	0.0475	0.0422	0.0330	0.0232	-
Skewness	0.8434	1.1727	1.3479	1.2184	-
Kurtosis	−0.0618	0.8768	2.4628	1.5078	-
W4 = 200					
Mean	0.0213	0.0245	0.0197	0.0071	0.0062
SD	0.0393	0.0351	0.0261	0.0215	0.0199
Skewness	0.9908	1.3799	1.6650	1.4585	1.6720
Kurtosis	−0.3018	0.9029	2.9319	2.2209	1.8339
W5 = 250					
Mean	0.0165	0.0211	0.0170	0.0030	−0.0043
SD	0.0335	0.0308	0.0242	0.0232	0.0310
Skewness	1.1137	1.3311	1.2920	−0.1065	−0.4814
Kurtosis	−0.2545	0.6427	1.8523	0.4632	0.8582

Table 2. The *Brent-HO* normality test of $\Delta\rho_{DCCA}$ for W1 to W5. Significance level of 95% (p-value < 0.05) rejects the null hypothesis of normality.

D'Agostino and Pearson's Normality Test					
Statistics	***n* = 4**	***n* = 8**	***n* = 16**	***n* = 32**	***n* = 64**
W1 = 50					
χ^2	24.1151	59.8950	171.8440	-	-
p-value	$\mathbf{5.80 \times 10^{-6}}$	$\mathbf{9.86 \times 10^{-14}}$	$\mathbf{4.84 \times 10^{-38}}$	-	-
W2 = 100					
χ^2	6.7952	7.873	0.9515	9.0797	-
p-value	**0.0335**	**0.0195**	0.6214	**0.0107**	-
W3 = 150					
χ^2	24.8080	46.5804	68.8323	54.3651	-
p-value	$\mathbf{4.10 \times 10^{-6}}$	$\mathbf{7.68 \times 10^{-11}}$	$\mathbf{1.13 \times 10^{-15}}$	$\mathbf{1.57 \times 10^{-12}}$	-
W4 = 200					
χ^2	32.8813	57.2596	88.2648	72.4758	79.9174
p-value	$\mathbf{7.24 \times 10^{-8}}$	$\mathbf{3.68 \times 10^{-13}}$	$\mathbf{6.82 \times 10^{-20}}$	$\mathbf{4.43 \times 10^{-18}}$	$\mathbf{3.89 \times 10^{-20}}$
W5 = 250					
χ^2	38.6335	52.6530	61.0372	2.7892	14.8160
p-value	$\mathbf{4.08 \times 10^{-9}}$	$\mathbf{3.69 \times 10^{-12}}$	$\mathbf{5.57 \times 10^{-14}}$	0.2479	**0.0010**

Thus, the contagion hypothesis can be tested for each $\Delta\rho_{DCCA}$ distribution. Table 3 depicts the significance test, where the *T*-test is applied to parametric (normal) distributions and the Wilcoxon signed-rank test for non-parametric (non-normal) distributions. One can note that there is evidence of a contagion predominance for time scales $n < 32$, which suggests short-term effect spillover when comparing P_1 and P_2. However, there is no strong evidence of the contagion effect for values of $n \geq 32$ days, which suggests that the market imbalances caused by COVID-19 did not affect the HO–Brent cross-correlation in the long term as much as the short term. Figure 2a–c confirms the alternative hypothesis ($\Delta\rho_{DCCA}(n) \neq 0$), where it is possible to notice a prevalence of $\Delta\rho_{DCCA}(n) > 0$ for the first 150 days of comparison. The $\Delta\rho_{DCCA}(n)$ overpasses the critical limits for most parts of the periods (see Table 4). On the other hand, from Figure 2d,e, one can observe that greater values of n and W tend to smooth the curves and have no clear pattern. However, for every time scale (n), the correlations are shown to be lower during the beginning of P_2 if compared to the same period in P_1, in addition to the lower $\Delta\rho_{DCCA}(n)$ in the last 50 days of the curves, which indicates that the HO–Brent fully recovered in terms of correlation after 200 days of the COVID-19 outbreak.

Table 3. The *Brent-HO* significance test of $\Delta\rho_{DCCA}$ for W1 to W5. Significance level of 95% (p-value < 0.05) rejects the null hypothesis of $\Delta\rho_{DCCA} = 0$.

***t*-Test or Wilcoxon Signed-Rank Test for Significance at Differences**					
Statistics	***n* = 4**	***n* = 8**	***n* = 16**	***n* = 32**	***n* = 64**
			W1 = 50		
Statistic	W = 2924	W = 1744	W = 2325	-	-
p-value	**1.03×10^{-29}**	**6.42×10^{-35}**	**2.67×10^{-32}**	-	-
			W2 = 100		
Statistic	W = 5951	W = 6600	t = 7.5491	W = 16,146	-
p-value	**2.37×10^{-18}**	**2.73×10^{-16}**	**7.94×10^{-13}**	0.9683	-
			W3 = 150		
Statistic	W = 7050	W = 4865	W = 4547	W = 15,694	-
p-value	**6.16×10^{-15}**	**4.25×10^{-22}**	**2.90×10^{-23}**	0.6706	-
			W4 = 200		
Statistic	W = 9763	W = 3956	W = 2472	W = 11,748	W = 15,046
p-value	**4.12×10^{-8}**	**1.62×10^{-25}**	**1.18e-31**	**0.0001**	0.3280
			W5 = 250		
Statistic	W = 11094	W = 3623	W = 3942	t = 2.0720	W = 12,846
p-value	**1.36×10^{-5}**	**7.81×10^{-27}**	**1.43×10^{-25}**	**0.0393**	**0.0043**

Table 4. The *Brent-HO* critical values of $\Delta\rho_{DCCA}$ with 90%, 95% and 99% confidence level (CL) for W1 to W5.

Critical Values	***n* = 4**	***n* = 8**	***n* = 16**	***n* = 32**	***n* = 64**
CL = 95%					
W1	0.1321	0.1464	0.2342	-	
W2	0.1229	0.1189	0.1111	0.0885	-
W3	0.1059	0.0971	0.0747	0.0363	-
W4	0.0863	0.0834	0.0651	0.0429	0.0500
W5	0.0751	0.0736	0.0584	0.0436	0.0511

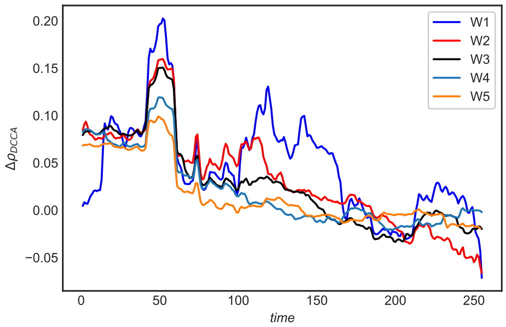

(**a**) $n = 4$

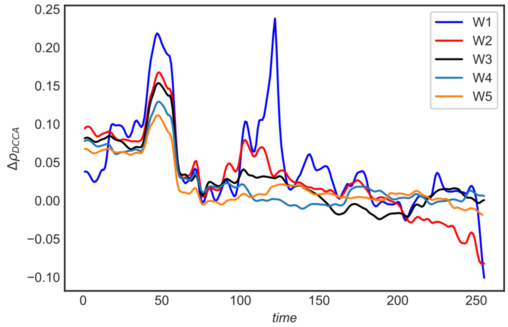

(**b**) $n = 8$

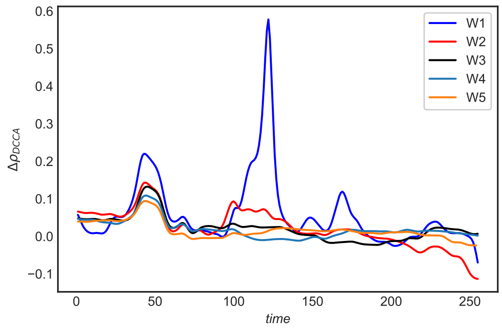

(**c**) $n = 16$

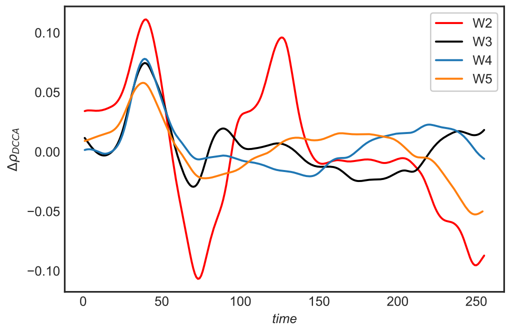

(**d**) $n = 32$

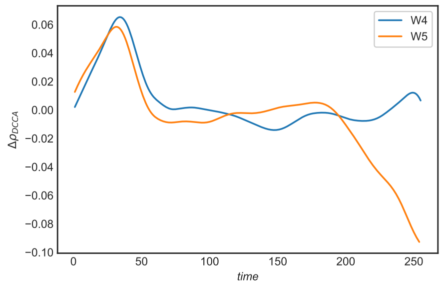

(**e**) n = 64

Figure 2. The *Brent-HO* $\Delta\rho_{DCCA}$ TS for different time scales (n).

4. Conclusions

This work employed Detrended Cross-Correlation Analysis in the study of the future contract price dynamics between the US diesel (HO) and Brent crude oil during the periods pre- and post-COVID-19. The results indicate that there is strong evidence of contagion in cross-correlation due to the initial impact of the pandemic, but the HO–Brent correlation fully recovered after approximately 200 days. However, lower time scales (n) are also sensitive to supply shortages in the short term and can be most reliable for agents that might not take long positions. Therefore, this indicates that, despite the pair being highly correlated, the initial global lack of crude oil demand generated by the lockdowns caused a fall in crude oil prices, but the same dynamics appeared in the US diesel market only after a delay.

Author Contributions: Conceptualization, S.A.D.; methodology, C.M.C.I.J. and S.A.D.; software, C.M.C.I.J.; formal analysis, C.M.C.I.J. and S.A.D.; writing—original draft preparation, C.M.C.I.J. and S.A.D.; writing—review and editing, C.M.C.I.J. and S.A.D.; visualization, C.M.C.I.J.; supervision, S.A.D. All authors have read and agreed to the published version of the manuscript.

Funding: This research received no external funding.

Institutional Review Board Statement: Not applicable.

Informed Consent Statement: Not applicable.

Data Availability Statement: Not applicable.

Acknowledgments: The authors wish to acknowledge the Institute of Mathematics and Computer Science of the University of São Paulo (ICMC-USP), CeMEAI-USP and MECAI-USP for the general and financial support.

Conflicts of Interest: The authors declare no conflicts of interest.

Abbreviations

The following abbreviations are used in this manuscript:

HO	Heating Oil (US Diesel)
TS	Time Series
SD	Standard Deviation
DCCA	Detrended Cross-Correlation Analysis
DFA	Detrended Fluctuation Analysis
P_1	First Period
P_2	Second Period
ARFIMA	Auto-Regressive Fractional Integrated Moving Average
H	Hurst Exponent

References

1. Hamilton, J. Oil and the Macroeconomy since World War II. *J. Political Econ.* **1983**, *91*, 228–248. [CrossRef]
2. Zhang, X.; Lai, K.; Wang, S. A new approach for crude oil price analysis based on Empirical Mode Decomposition. *Energy Econ.* **2008**, *30*, 905–918. [CrossRef]
3. Sauter, R.; Awerbuch, S. Oil price volatility and economic activity: A survey and literature review. *Iea Res. Pap.* **2003**, *28*, 550–577.
4. Lu, Q.; Li, Y.; Chai, J.; Wang, S. Crude oil price analysis and forecasting: A perspective of "new triangle". *Energy Econ.* **2020**, *87*, 104721. [CrossRef]
5. Ji, Q.; Guo, J. Oil price volatility and oil-related events: An Internet concern study perspective. *Appl. Energy* **2015**, *137*, 256–264. [CrossRef]
6. Matutinović, I. Oil and the political economy of energy. *Energy Policy* **2009**, *37*, 4251–4258. [CrossRef]
7. David, S.; Inácio, C.; Quintino, D.; Machado, J. Measuring the Brazilian ethanol and gasoline market efficiency using DFA-Hurst and fractal dimension. *Energy Econ.* **2020**, *85*, 104614. [CrossRef]
8. Chen, H.; Liao, H.; Tang, B.; Wei, Y. Impacts of OPEC's political risk on the international crude oil prices: An empirical analysis based on the SVAR models. *Energy Econ.* **2016**, *57*, 42–49. [CrossRef]
9. Guedes, E.; Zebende, G. DCCA cross-correlation coefficient with sliding windows approach. *Phys. A Stat. Mech. Appl.* **2019**, *527*, 121286. [CrossRef]
10. Tilfani, O.; Ferreira, P.; Boukfaoui, M. Dynamic cross-correlation and dynamic contagion of stock markets: A sliding windows approach with the DCCA correlation coefficient. *Empir. Econ.* **2021**, *60*, 1127–1156. [CrossRef]
11. Ferreira, P.; Kristoufek, L.; Area Leão Pereira, E. DCCA and DMCA correlations of cryptocurrency markets. *Phys. A Stat. Mech. Appl.* **2020**, *545*, 123803. [CrossRef]
12. Wang, B.; Wei, Y.; Xing, Y.; Ding, W. Multifractal detrended cross-correlation analysis and frequency dynamics of connectedness for energy futures markets. *Phys. A Stat. Mech. Appl.* **2019**, *527*, 121194. [CrossRef]
13. Prass, T.; Pumi, G. On the behavior of the DFA and DCCA in trend-stationary processes. *J. Multivar. Anal.* **2021**, *182*, 104703. [CrossRef]
14. He, L.; Chen, S. Multifractal Detrended Cross-Correlation Analysis of agricultural futures markets. *Chaos Solitons Fractals* **2011**, *44*, 355–361. [CrossRef]
15. Cai, Y.; Lu, X.; Ren, Y.; Qu, L. Exploring the dynamic relationship between crude oil price and implied volatility indices: A MF-DCCA approach. *Phys. A Stat. Mech. Appl.* **2019**, *536*, 120973. [CrossRef]
16. Paiva, A.; Rivera-Castro, M.; Andrade, R. DCCA analysis of renewable and conventional energy prices. *Phys. A Stat. Mech. Appl.* **2018**, *490*, 1408–1414. [CrossRef]
17. Malik, A.; Brönnimann, S. Factors affecting the inter-annual to centennial timescale variability of Indian summer monsoon rainfall. *Clim. Dyn.* **2018**, *50*, 4347–4364. [CrossRef]
18. Lin, M.; Wang, G.; Xie, C.; Stanley, H. Cross-correlations and influence in world gold markets. *Phys. A Stat. Mech. Appl.* **2018**, *490*, 504–512. [CrossRef]

19. Zebende, G.; Silva, M.; Filho, A. DCCA cross-correlation coefficient differentiation: Theoretical and practical approaches. *Phys. A Stat. Mech. Appl.* **2013**, *392*, 1756–1761. [CrossRef]
20. Ferreira, P.; Dionísio, A.; Guedes, E.; Zebende, G. A sliding windows approach to analyse the evolution of bank shares in the European Union. *Phys. A Stat. Mech. Appl.* **2018**, *490*, 1355–1367. [CrossRef]
21. David, S.; Inacio, C., Jr.; Nunes, R.; Machado, J. Fractional and fractal processes applied to cryptocurrencies price series. *J. Adv. Res.* **2021**, *32*, 85–98. [CrossRef] [PubMed]
22. Valentim, C.; Inacio, C.; David, S. Fractal Methods and Power Spectral Density as Means to Explore EEG Patterns in Patients Undertaking Mental Tasks. *Fractal Fract.* **2021**, *5*, 225. [CrossRef]
23. Kristoufek, L.; Vosvrda, M. Commodity futures and market efficiency. *Energy Econ.* **2014**, *42*, 50–57. [CrossRef]
24. David, S.; Machado, J.; Trevisan, L.; Inácio, C., Jr.; Lopes, A. Dynamics of commodities prices: Integer and fractional models. *Fundam. Inform.* **2017**, *151*, 389–408. [CrossRef]
25. David, S.; Machado, J.; Inácio, C.; Valentim, C. A combined measure to differentiate EEG signals using fractal dimension and MFDFA-Hurst. *Commun. Nonlinear Sci. Numer. Simul.* **2020**, *84*, 105170. [CrossRef]
26. David, S.; Inácio, C.; Machado, J. Quantifying the Predictability and Efficiency of the Cointegrated Ethanol and Agricultural Commodities Price Series. *Appl. Sci.* **2019**, *9*, 5303. [CrossRef]
27. Ayadi, O.; Williams, J.; Hyman, L. Fractional dynamic behavior in Forcados Oil Price Series: An application of detrended fluctuation analysis. *Energy Sustain. Dev.* **2009**, *13*, 11–17. [CrossRef]
28. Shang, P.; Lu, Y.; Kamae, S. Detecting long-range correlations of traffic time series with multifractal detrended fluctuation analysis. *Chaos Solitons Fractals* **2008**, *36*, 82–90. [CrossRef]
29. Teng, Y.; Shang, P. Detrended fluctuation analysis based on higher-order moments of financial time series. *Phys. A Stat. Mech. Appl.* **2018**, *490*, 311–322. [CrossRef]
30. Kristoufek, L. Testing power-law cross-correlations: Rescaled covariance test. *Eur. Phys. J.* **2013**, *86*, 1–11. [CrossRef]
31. Peng, C.; Buldyrev, S.; Havlin, S.; Simons, M.; Stanley, H.; Goldberger, A. Mosaic organization of DNA nucleotides. *Phys. Rev. E* **1994**, *49*, 1685–1689. [CrossRef] [PubMed]
32. Shieh, S. Long Memory and sampling frequencies: Evidence in stock index futures markets. *Int. J. Theor. Appl. Financ.* **2006**, *9*, 787–799. [CrossRef]
33. Carbone, A. Detrending moving average algorithm: A brief review. *Dimension* **2009**, *49*, 59.
34. Simonsen, I.; Hansen, A.; Nes, O. Determination of the Hurst exponent by use of wavelet transforms. *Phys. Rev. E* **1998**, *58*, 2779. [CrossRef]
35. Mandelbrot, B. Statistical methodology for nonperiodic cycles: From the covariance to R/S analysis. *Ann. Econ. Soc. Meas.* **1972**, *1*, 259–290.
36. Mandelbrot, B.; Wallis, J. Robustness of the rescaled range R/S in the measurement of noncyclic long run statistical dependence. *Water Resour. Res.* **1969**, *5*, 967–988. [CrossRef]
37. Podobnik, B.; Stanley, H. Detrended cross-correlation analysis: A new method for analyzing two nonstationary time series. *Phys. Rev. Lett.* **2008**, *100*, 084102. [CrossRef] [PubMed]
38. Podobnik, B.; Jiang, Z.; Zhou, W.; Stanley, H. Statistical tests for power-law cross-correlated processes. *Phys. Rev. E Stat. Nonlinear Soft Matter Phys.* **2011**, *84*, 066118. [CrossRef] [PubMed]
39. Zebende, G. DCCA cross-correlation coefficient: Quantifying level of cross-correlation. *Phys. A Stat. Mech. Appl.* **2011**, *390*, 614–618. [CrossRef]
40. Guedes, E.; Brito, A.; Filho, F.; Fernandez, B.; Castro, A.; Silva Filho, A.; Zebende, G. Statistical test for $\Delta\rho$DCCA cross-correlation coefficient. *Phys. A Stat. Mech. Appl.* **2018**, *501*, 134–140. [CrossRef]
41. Silva, M.; Area Leão Pereira, É.; Silva Filho, A.; Castro, A.; Miranda, J.; Zebende, G. Quantifying the contagion effect of the 2008 financial crisis between the G7 countries (by GDP nominal). *Phys. Stat. Mech. Appl.* **2016**, *453*, 1–8. [CrossRef]
42. D'Agostino, R.; Pearson, E. Tests for departure from normality. Empirical results for the distributions of b2 and b1. *Biometrika* **1973**, *60*, 613–622. [CrossRef]
43. D'Agostino, R. An Omnibus Test of Normality for Moderate and Large Size Samples. *Biometrika* **1971**, *58*, 341. [CrossRef]
44. French, M. *Hurricane Ida Disrupted Crude Oil Production and Refining Activity*; U.S. Energy Information Administration (EIA): Washington, DC, USA, 2021. Available online: https://www.eia.gov/todayinenergy/detail.php?id=49576 (accessed on 14 April 2022).